

Biosorption of Multifold Toxic Heavy Metal Ions from Aqueous Water onto Food Residue Eggshell Membrane Functionalized with Ammonium Thioglycolate

Sha Wang, Minghong Wei, and Yuming Huang*

State Key Laboratory Breeding Base of Eco-Environments and Bio-Resources of the Three Gorges Reservoir Region, College of Chemistry and Chemical Engineering, Southwest University, Chongqing 400715, China

S Supporting Information

ABSTRACT: A new biosorbent material from eggshell membrane was synthesized through thiol functionalization, which is based on the reduction of disulfide bonds in eggshell membrane by ammonium thioglycolate. The thiol-functionalized eggshell membrane was characterized, and its application as an adsorbent for removal of Cr(VI), Hg(II), Cu(II), Pb(II), Cd(II), and Ag(I) from aqueous water has been investigated. The experimental results revealed that the adsorption abilities of the thiol-functionalized eggshell membrane toward Cr(VI), Hg(II), Cu(II), Pb(II), Cd(II), and Ag(I) improved 1.6-, 5.5-, 7.7-, 12.4-, 12.7-, and 21.1-fold, respectively, compared with that of the eggshell membrane control. The adsorption mechanism and adsorption performance, including the adsorption capacity and the kinetics of the thiol-functionalized eggshell membrane for the target heavy metals, were investigated. The effects of solution pH, coexisting substances, and natural water matrices were studied. The thiol-functionalized eggshell membrane can be used as column packing to fabricate a column for real wastewater purification.

KEYWORDS: biosorption, eggshell membrane, biosorbent, thiol functionalization, heavy metal ions, removal, food residues

INTRODUCTION

With the development of tannery, chemical manufacturing, mining industries, and other industrial activities, environmental contamination and human exposure to heavy metals have attracted tremendous attention.^{1–3} Although some heavy metals (e.g., copper and selenium) are essential for maintaining the metabolism of the human body as trace elements, they can lead to poisoning at higher concentrations.^{4,5} Furthermore, some heavy metals (e.g., lead, chromium, and mercury) are serious threats to public health and ecosystems even at low concentrations because of bioaccumulation and biomagnification.⁶ Thus, efficient removal of the toxic metal ions in water has been an actively pursued goal of water treatment. Various methods, including adsorption,⁷ precipitation,⁸ ion exchange,⁹ and electrochemical techniques,¹⁰ have been developed for the elimination of toxic heavy metals from water. Among these, adsorption is one of the most attractive methods because of its simplicity and effectiveness and, thus, seems to be superior to other technologies for water treatment.^{11,12}

In recent years, biosorption has received an increasing amount of attention for the removal and recovery of heavy metals from aqueous solutions because biomaterials are abundant, inexpensive, and available in nature and because of minimization of secondary wastes.^{13–15} However, they usually suffer from disadvantages, including poor metal removal ability and slow process kinetics. Thus, it is highly desirable to develop inexpensive adsorbents with a strong affinity for toxic metal ions. Surface functionalization has been proven to be an effective way to create such a promising adsorbent because functional groups not only can provide binding sites for the removal of the metal ions from aqueous solutions but also can improve the adsorption properties. In fact, surface functional-

ization with carboxylate, hydroxyl, amide, and amine groups on the surface of the biosorbents has been reported for heavy metal ion removal.^{16,17}

The thiol group is an excellent ligand because of its strong affinity for various heavy metal ions as the result of Lewis acid–base interactions.^{18,19} However, no report of the investigation of the thiol group-functionalized eggshell membrane (ESM) for adsorption removal of the toxic metal ions has been published. There are four reasons for us to select ESM as a biomaterial. First, it can be readily obtained almost anywhere and in large quantities as an industrial waste natural product at almost no cost.²⁰ Second, as one kind of food residue, ESM has surface functional groups, such as amines, amides, and carboxylic groups. Third, as a light pink double-layer membrane inside eggshells, ESM is mainly composed of biological molecules and highly cross-linked protein fibers with excellent gas and water permeability and intricate lattice network construction. Fourth, many disulfide bridges exist, part of a cystine residue in ESM.²¹ Under alkaline conditions, it is easy to realize the reductive cleavage of disulfide bonds into thiol groups.²²

The objective of this study was to investigate the feasibility of using thiol functionalized ESM (TESM) as a biosorbent for the removal of toxic heavy metals from aqueous media. TESHM was prepared by using a facile and simple reduction of the disulfide bond in keratin by ammonium thioglycolate. The adsorption mechanism and adsorption performance, including the

Received: December 5, 2012

Revised: May 9, 2013

Accepted: May 11, 2013

Published: May 11, 2013

adsorption capacity and the kinetics of the TESM for toxic heavy metals, were investigated.

EXPERIMENTAL PROCEDURES

Reagents and Chemicals. All the chemicals were of analytical grade. Thioglycolic acid was purchased from Kelong Chemical Reagents Co. (Chengdu, Sichuan, China), and the others were purchased from Chongqing Chemical Reagents Co. (Chongqing, China). Ultrapure water was used. The pH of the solution was adjusted by using 0.1 M NaOH or 0.1 M HNO₃.

Preparation of Thiol-Functionalized Eggshell Membrane (TESM). Fresh eggshell was obtained from the canteen of Southwest University, and ESM can be peeled off easily. ESM was washed with water. The cleaned ESM was immersed in a 0.5 M HCl solution for 12 h to remove the residual impurities.²³ Then it was washed with adequate ultrapure water. In succession, ESM was dried at 80 °C and cut into small pieces with scissors for further use. To prepare the TESM, 1 g of treated ESM was immersed in 400 mL of a basic ammonium thioglycolate solution, which was prepared by adding 40 mL of thioglycolic acid and 80 mL of ammonia. The mixture was kept for 12 h at room temperature for the redox reaction between the disulfide bond in keratin on ESM and ammonium thioglycolate and then washed with ultrapure water. The washed TESM product was finally dried at 50 °C for 2 h and preserved in a desiccator for characterization and the adsorption test.

Instrumentation. Scanning transmission electron microscopy (SEM) images were taken on a Hitachi model S4800 field emission scanning electron microscope (Hitachi, Tokyo, Japan) with an accelerating voltage of 20 kV. The Raman spectra were recorded on a Bruker RFS/S 100 apparatus (Bruker, Saarbrücken, Germany). An XSAM800 X-ray photoelectron spectrometer (Kratos, Manchester, Britain) was used for the surface analysis of the adsorbent. A Z-2000 Series Polarized Zeeman atomic absorption spectrophotometer (Hitachi) was employed for copper, cadmium, silver, lead, calcium, and magnesium. A UV-vis measurement of Cr(VI) was performed on a UV-2450 Shimadzu (Suzhou, China) spectrophotometer. An AFS-230E HG-AFS (hydride generation, double-channel atomic fluorescence spectrometer) (Beijing Haiguang Instrument Ltd., Beijing, China) was used for mercury. TOC measurement was performed with a Hach IL TOC-550 Total Organic Carbon Analyzer.

Analytical Methods for the Determination of Metal Ion Concentrations. The Hg(II) concentration in an aqueous solution was measured using HG-AFS following the published procedure.²⁴ Measurements of Cu(II), Pb(II), Cd(II), Ag(I), Ca(II), Mg(II), and Cr followed standard methods.^{25–28} Different certified reference materials, including GBW(E)080397 for Cu(II), GBW(E)080181 for Cr(VI), GBW(E)080363 for Cd(II), GBW(E)080176 for Ag(I), GBW(E)080124 for Hg(II), and GBW(E)080003 for Pb(II) (Institute of Reference Materials, Beijing, China), were used to validate the used analytical method. Good agreement was achieved between the analytical results of the certified reference and the certified values, with differences of <1.0%. The precision of the analytical procedures, expressed as the relative standard deviation (RSD), was <4.0%. In different experiments, blanks were run, and corrections were applied if necessary. Controls included heavy metal ion working solutions in the absence of adsorbent for the examination of any loss of target ions other than to TESM sorption, such as sorption to the glass containers. Such losses were found to be negligible.

Batch Adsorption Experiments. Heavy metal ions adsorption experiments were conducted by batch method. All experiments were performed in a 100 mL stoppered conical flask. A total of 50 mL of each solution was treated with 0.05 g of TESM and shaken at 180 rpm in a constant-temperature incubator; 0.1 M HNO₃ and 0.1 M NaOH solutions were used for pH adjustment. Individual experiments were conducted to determine the maximal binding capacity with each of the heavy metals. Note that the batch adsorption experiments were operated in single-component working solutions that contained only one target metal ion. The uptake capacity of TESM for heavy metals was determined by analyzing the metal concentration of the solution

before and after adsorption. To establish the accuracy, reliability, and reproducibility of the collected data, all of the results were performed in duplicate, and the data were recorded as an average value. The amount of heavy metals taken up on the adsorbent was calculated according to the equation

$$q_t = (C_0 - C_t)V/m$$

where q_t is the amount (milligrams per gram) adsorbed per gram of adsorbent at time t (minutes), C_0 and C_t are the initial sorbate concentration and the sorbate concentration at time t in the solution, respectively (both in milligrams per liter), m is the mass of the adsorbent used (grams), and V is the volume of the solution (milliliters).

For the adsorption kinetic studies, at pH =3.0 for Cr(VI) or pH =6.0 for Hg(II), Cu(II), Pb(II), Cd(II), and Ag(I), 50 mg of TESM was added to 50 mL of a target heavy metal ion solution with contact times ranging from 0 to 24 h. The initial concentrations of Hg(II), Cr(VI), Ag(I), Cu(II), Cd(II), and Pb(II) were 150, 100, 100, 50, 50, and 50 mg/L, respectively. The flasks were shaken at 180 rpm and 30 °C. At specific time intervals, samples were taken for analysis of metal ion concentration. Each data point was obtained from an individual flask, and therefore, no correction was necessary because of the withdrawal of the sampling volume.

For the adsorption equilibrium studies, at pH =3.0 for Cr(VI) or pH =6.0 for Hg(II), Cu(II), Pb(II), Cd(II), and Ag(I), 50 mg of TESM was added to 50 mL of different concentrations of the target metal ions solution, and the flasks were shaken at 180 rpm in a thermostatic shaker at 30 °C for 24 h. After adsorption, the metal ion concentrations of the samples were analyzed.

To investigate the effect of pH, 50 mg of TESM was added to 50 mL of the target metal ions solution with pH values ranging from 1.0 to 9.0. The initial concentrations of Hg(II), Cr(VI), Ag(I), Cu(II), Cd(II), and Pb(II) were 150, 100, 100, 50, 50, and 50 mg/L, respectively, and the flasks were shaken at 180 rpm and 30 °C for 24 h. After adsorption, the metal ion concentrations of the samples were analyzed.

Effect of Natural Water Matrices. Different water samples were selected to investigate the adsorbability of TESM in natural matrices. Ultrapure water was prepared in our laboratory. A tap water sample was collected from our laboratory after the tap had been open for 10 min. A river water sample was obtained from the Jialing River. To assess the effect of natural water matrices, at pH =3.0 for Cr(VI) or pH =6.0 for Hg(II), Cu(II), Pb(II), Cd(II), and Ag(I), 50 mg of TESM was added to 50 mL of the spiked water samples. The spiked concentrations of Hg(II), Cr(VI), Ag(I), Cu(II), Cd(II), and Pb(II) were 150, 100, 100, 50, 50, and 50 mg/L, respectively, and the flasks were shaken at 180 rpm in a thermostatic shaker at 30 °C for 24 h. After adsorption, the metal ion concentrations of the samples were analyzed, and then the samples were used to evaluate the effects of different matrices on the removal of target heavy metal ions.

Breakthrough Experiments for Practical Wastewater Purification. Five industrial wastewaters were used to evaluate the adsorption ability of TESM or ESM through a nonstop column breakthrough experiment for practical application. Among them, four electroplating wastewaters, denoted samples I–IV, mainly containing 3.51 mg/L Cu(II), 5.54 mg/L Cr(VI), 8.10 mg/L Pb(II), and 5.93 mg/L Ag(I), were obtained from the effluent of four electroplating factories. Another industrial wastewater with 110.50 mg/L Cr(VI), denoted sample V, was collected from the effluent of a factory producing Na₂CrO₄. The breakthrough experiments were performed on a short column by modifying a C18 cartridge (0.5 g, 3 mL, polypropylene) purchased from Supelco Corp. The C18 packing material was removed, and 250 mg of biosorbents was packed into the cartridge with TESM or ESM as column packing. A model SHZ-3 (III) vacuum pump (Yuhua Instrument Co. Ltd., Zhengzhou, China) was used to add feed solutions to the top of the column at a rate of 3.0 mL/min. The maximal 3500 BV (bed volume, which refers to the volume of the solution equivalent to the volume of the adsorbent in the column) practical wastewater solution was run for the loading test. The filtrate samples were manually collected and used for analysis of

target heavy metals. The breakthrough curves were then obtained from the analytical results of target heavy metals.

RESULTS AND DISCUSSION

Characterizations of TESM. The TESM was synthesized on the basis of the reduction of disulfide bonds in ESM by ammonium thioglycolate. The introduction of an SH group onto the ESM surface was confirmed by the results of the Raman spectra. As shown in Figure 1, the stretching signature

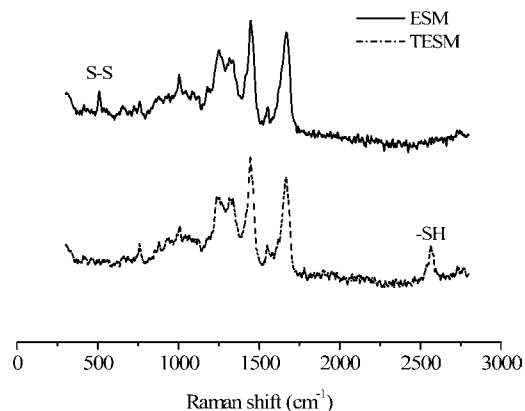
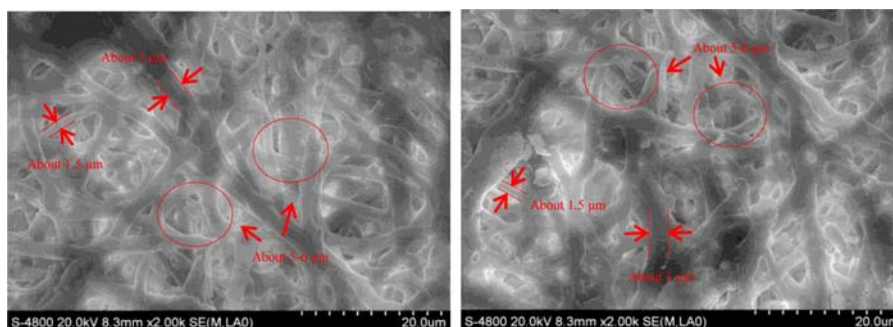


Figure 1. Raman spectra of ESM and TESM.

of the S–S bond appears clearly at $\sim 510\text{ cm}^{-1}$ in ESM,²⁹ which disappears after ammonium thioglycolate treatment of ESM. Meanwhile, the appearance of the thiol group was found in the prepared product, exhibiting significant peaks at 2565 cm^{-1} , which is attributed to the S–H stretching mode.³⁰ The surface morphologies of the as-prepared biosorbents in Figure 2 reveal that thiol functionalization to create TESM is a gentle process: it leaves the original macroporous network structure of ESM that consists of highly cross-linked protein fibers ($\sim 1.5\text{--}3\text{ }\mu\text{m}$ diameter). The presence of macropores with pore sizes of $\sim 5\text{--}6\text{ }\mu\text{m}$ is evident, which is beneficial to mass transfer as a sorbent. The BET surface area of ESM remained almost unchanged after thiol functionalization. However, the total pore volume decreased slightly. This result is reasonable because thiol functionalization of ESM introduces the SH groups into ESM through chemical reaction. Also, the determination of the ζ potential indicates that TESM and ESM are positively charged at low pH and negatively charged at high pH, with the points of zero charge (PZC) at pH values of 8.30 and 5.45,



(A)

(B)

Figure 2. SEM images of ESM (A) and TESM (B).

respectively. Clearly, TESM has a more positively charged surface than ESM because of the protonation of the thiol group.

Effect of pH. To investigate the effect of pH on adsorption behavior of heavy metals and eliminate the interference of precipitation, a disparate pH range was chosen for different target ions. For Cr(VI), an initial pH value from 1 to 9 was selected, but for Cu(II), Hg(II), Ag(I), Pb(II), and Cd(II), a pH of >6 was not considered to prevent the heavy metals from precipitating. As shown in Figure 3, the capacity of TESM to

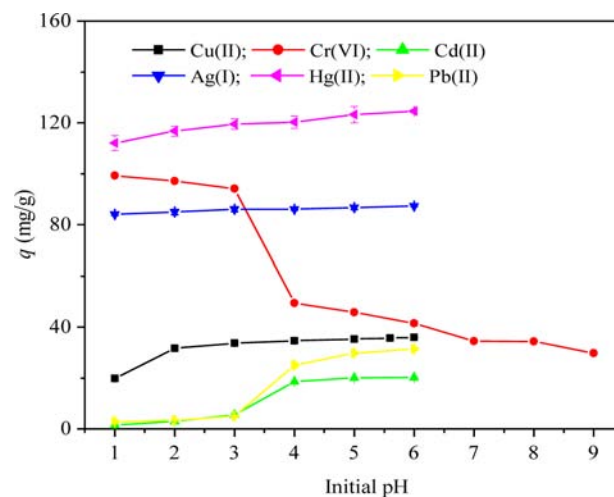


Figure 3. Effect of initial solution pH.

target toxic metal ions showed different pH dependencies. For Cu(II), Hg(II), Ag(I), Pb(II), and Cd(II), the adsorption capacity increased with increasing pH in the studied pH range: $\text{Hg(II)} > \text{Ag(I)} > \text{Cu(II)} > \text{Pb(II)} \approx \text{Cd(II)}$. This could be explained by Pearson's theory that soft ligands, like the thiol group,³¹ are more likely to bind with soft metals, such as Hg(II) and Ag(I), to form complexes while Cu(II), Cd(II), and Pb(II) have larger hardness parameters³² and are considered hard–medium–soft metals, which leads to the weaker binding to thiol groups. Moreover, they are less thermodynamically favorable than Hg(II) in reacting with thiol groups;³³ thus, the adsorption capacities of TESM for Hg(II) and Ag(I) are much higher than those of Cu(II), Pb(II), and Cd(II) ions. In addition, the $\text{p}K_a$ of the SH group is reported to be 9.65;¹⁸ under acidic conditions, the SH group was protonated to form the positively charged sites and electrostatic repulsion occurs between metal ions and the positive surface of the TESM,

leading to the increase in the level of metal ion adsorption by TESM with the increase in pH. Therefore, we chose pH 6 as the optimal pH for the metal ions studied here.

The effect of pH on Cr(VI) adsorption over the pH range of 1.0–9.0 was investigated. The highest level of Cr(VI) adsorption was observed at pH 1.0. The level of adsorption decreased sharply with the increase in solution pH from 3.0 to 4.0. At pH >4.0, the level of adsorption decreased slowly with an increase in solution pH. The effect of solution pH can be tentatively explained by considering the surface charge of the adsorbents and the degree of ionization of the sorbates. The surface of TESM is covered with thiol groups and amino groups that vary in form at different pH levels. Under strongly acidic conditions, thiol groups and amino groups were protonated to form the positively charged sites and electrostatic attraction occurred between HCrO_4^- and positively charged sites on the surface of TESM, leading to the increase in the efficiency of removal. With an increasing pH value, the concentration of H^+ decreases while the concentration of OH^- increases, leading to competition with HCrO_4^- and thus resulting in the decrease in the level of adsorption.

Adsorption Kinetics. The kinetics of adsorption is one of the most important parameters to describe the efficiency of adsorption. The effect of contact time on the adsorption of various ions is shown in Figure 4. The results of the kinetics of

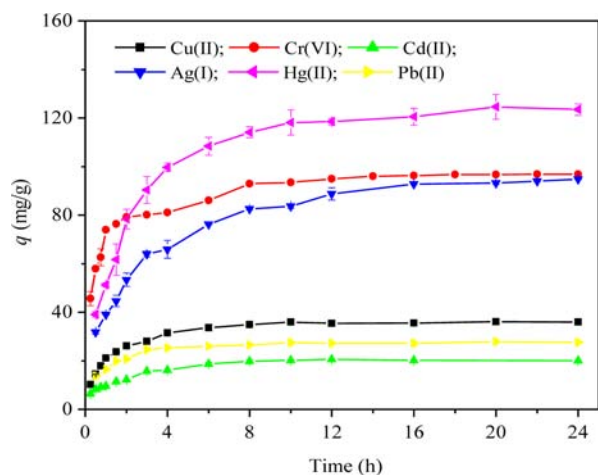


Figure 4. Adsorption kinetics of metal ions by TESM.

removal of target heavy metal ions on TESM suggested a rapid initial uptake and a subsequent stable stage (Figure 4). For example, the adsorption process is fast for the first 3 h, and uptake capacities of 50% can be reached for the target metal ions. With an increase in the contact time, the adsorption of TESM for Cu(II), Cd(II), and Pb(II) reached equilibrium at 4 h. For Cr(VI), Hg(II), and Ag(I), the adsorption equilibrium time was ~8 h. Pseudo-first-order³⁴ and pseudo-second-order³⁵ models were used to fit the experimental data and evaluate the adsorption kinetic process.

$$\ln(q_e - q_t) = \ln q_e - k_1 t \quad (1)$$

$$t/q_t = 1/(k_2 q_e^2) + t/q_e \quad (2)$$

where q_e is the adsorption capacity (milligrams per gram) at equilibrium, q_t is the adsorption capacity (milligrams per gram) at time t , and k_1 (inverse minutes) and k_2 (grams per milligram per minute) stand for the adsorption rates of pseudo-first-order

and pseudo-second-order models, respectively. The values of correlation coefficients indicated a better fit of the pseudo-second-order model with the experimental data than of the pseudo-first-order model. The calculated q_e values are in agreement with the theoretical ones, and the plots show quite good linearity with r^2 values of >0.99. Therefore, the adsorption kinetics follows the pseudo-second-order model, suggesting a chemisorption process.

Adsorption Isotherms. The adsorption capacities for metal ions sharply increased with an increase in the equilibrium concentrations in the low-concentration region and then increased slowly at concentrations of >10 mg/L for TESM (Figure 5). The adsorption isotherm is important for

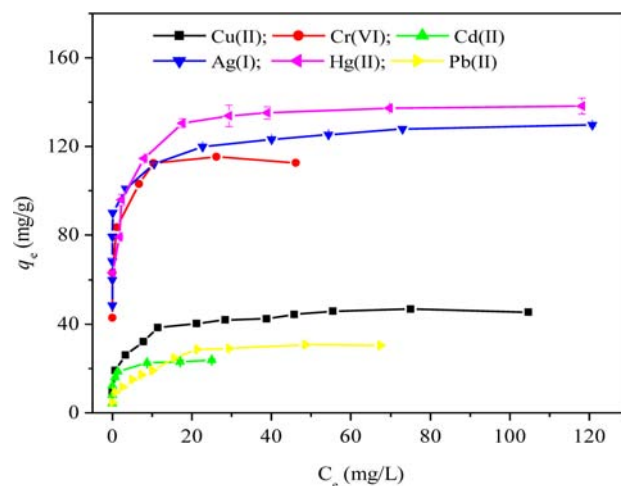


Figure 5. Adsorption isotherms of various ions at different concentrations.

determining the adsorption behavior of an adsorbent. The Langmuir,³⁶ Freundlich,³⁷ and Dubinin–Rudushevich (D–R)³⁸ isotherm equations were employed to fit the experimental data:

$$C_e/q_e = C_e/q_{\max} + 1/(q_{\max} b) \quad (3)$$

$$\log q_e = \log k_f + (1/n) \log C_e \quad (4)$$

$$\ln q_e = \ln q_{\max} - k_D \varepsilon^2 \quad (5)$$

where C_e denotes the equilibrium concentration of the metal ions (milligrams per liter), q_e is the equilibrium adsorption capacity (milligrams per gram), q_{\max} represents the maximal adsorption capacity of the adsorbent (milligrams per gram), b is the Langmuir constant related to the energy of adsorption (liters per milligram), k_f and n are the constants of the Freundlich adsorption model correlated to the relative adsorption capacity and the adsorption intensity, respectively, k_D is the constant related to the adsorption energy (square moles per square kilojoules), and ε is the Polanyi potential that is equal to $RT \ln(1 + 1/C_e)$, where R is the gas constant and T is the absolute temperature (kelvin).

As one can see from Table 1, the Langmuir model effectively described the adsorption data with all $r^2 > 0.99$, suggesting a better fit of the Langmuir isotherm with the experimental data compared to those with the Freundlich and D–R isotherms, which demonstrates the adsorption process occurs on a homogeneous surface of the adsorbent and each binding site can be occupied only once. The maximal equilibrium

Table 1. Relevant Parameters of Freundlich, Langmuir, and Dubinin–Ruduschevich Adsorption Isotherms

adsorbent	target	Langmuir model			Freundlich model			Dubinin–Ruduschevich model		
		b (L/mg)	q_{\max} (mg/g)	r^2	n	k_f	r^2	q_{\max} (mg/g)	k_D (mol ² /kJ ²)	r^2
TESM	Cr(VI)	6.769	113.64	0.9996	11.682	86.099	0.8602	116.90	0.0035	0.9674
	Hg(II)	1.286	138.89	0.9998	8.026	83.599	0.8618	146.40	0.0038	0.9562
	Ag(I)	0.713	129.87	0.9996	18.248	99.839	0.9626	123.10	0.0011	0.8075
	Cu(II)	0.447	46.73	0.9982	5.470	21.842	0.9505	44.61	0.0070	0.9421
	Cd(II)	5.342	23.70	0.9994	9.643	17.406	0.9529	25.00	0.0025	0.9848
	Pb(II)	0.250	32.47	0.9907	3.327	9.786	0.9546	32.20	0.0069	0.9133
ESM	Cr(VI)	0.543	43.67	0.9945	6.090	17.559	0.9729	30.32	0.0045	0.8853
	Hg(II)	0.199	21.51	0.9596	2.079	31.003	0.7621	29.32	0.0118	0.8229
	Ag(I)	0.915	5.89	0.9985	3.200	2.556	0.8435	6.31	0.0058	0.8672
	Cu(II)	0.457	5.37	0.9412	1.547	2.092	0.8276	8.50	0.0166	0.9393
	Cd(II)	2.862	1.73	0.9913	2.870	0.936	0.7451	2.49	0.0063	0.8252
	Pb(II)	2.414	2.43	0.9993	3.092	1.264	0.7963	3.75	0.0056	0.9133

Table 2. Adsorption Capacities of the Target Heavy Metal Ions by TESM from Different Water Samples

matrix	TOC (mg/L)	Mg ²⁺ (mg/L)	Ca ²⁺ (mg/L)	adsorption capacity (mg/g \pm SD, $n = 2$)					
				Cr(VI)	Hg(II)	Ag(I)	Cu(II)	Cd(II)	Pb(II)
ultra pure water	ND ^a	ND ^a	ND ^a	91.68 \pm 0.06	119.09 \pm 6.16	92.20 \pm 0.27	31.50 \pm 0.02	19.16 \pm 0.97	26.93 \pm 1.46
tap water	2.64	8.20	61.40	89.10 \pm 0.35	122.55 \pm 8.07	94.27 \pm 0.53	30.57 \pm 0.97	17.16 \pm 0.47	23.72 \pm 1.03
river water	3.32	9.15	62.05	82.42 \pm 0.14	120.45 \pm 0.06	95.07 \pm 0.08	25.30 \pm 0.74	16.98 \pm 0.46	18.95 \pm 0.14

^aNot detected.

adsorption capacities (q_{\max}) of TESM, obtained by the Langmuir model, toward Cr(VI), Hg(II), Cu(II), Pb(II), Cd(II), and Ag(I) were 113.64, 138.89, 46.73, 32.47, 23.70, and 129.87 mg/g, respectively (Table 1). Compared with the ESM control, the adsorption capacities of TESM toward Cr(VI), Hg(II), Cu(II), Pb(II), Cd(II), and Ag(I) increased 1.6-, 5.5-, 7.7-, 12.4-, 12.7-, and 21.1-fold, respectively. This suggests the importance of the thiol group for the removal of target toxic metal ions. Also, the adsorption capacity of the TESM is compared with the values for thiol-functionalized adsorbents and other biosorbents for the removal of target heavy metal ions reported in the literature. For thiol-functionalized adsorbents, except for thiol-functionalized hierarchically porous silica for Cu(II), Cd(II), and Pb(II), the maximal adsorption capacity obtained with TESM is much higher than those obtained with many other adsorbents, such as thio-modified cellulose resins,³⁹ thiol-modified silica gel,⁴⁰ thiol-functionalized silica/polystyrene composite,⁴¹ and thiol-modified Fe₃O₄/SiO₂.⁴² In addition, the results indicate that its adsorption capacity is much greater than that of the same ion for some other biosorbents reported previously.

Effect of Other Coexisting Substances. The effect of other commonly coexisting substances in aqueous media, including metal ions (Na⁺, K⁺, Mg²⁺, Ca²⁺, and Fe³⁺), typical anions (Cl⁻, NO₃⁻, SO₄²⁻, and PO₄³⁻, 1 g/L each), and natural organic matter (NOM) with Aldrich humic acid (HA) as a model, was also investigated. The effect of coexisting substances was performed by mixing 50 mg of adsorbent and coexisting substances in 50 mL of the target toxic heavy metal ion solution. The experimental results indicated that the presence of Na⁺ or K⁺ ions, even at a concentration (500 mg/L) much higher than those of the target heavy metal ions, reduced the extent of removal of the target heavy metal ions by <15%. Other higher-valence ions, such as Mg²⁺, Ca²⁺, or Fe³⁺, had a more suppressive effect on the adsorption of the target heavy

metal ions. Although their affinity for the thiol group is weak, they could still bind with a portion of the adsorption sites on the surface of TESM and compete with target ions to bind with TESM. Results also indicated the positive role of PO₄³⁻ in the removal of Hg(II), Cu(II), Pb(II), Cd(II), and Ag(I) as a result of the cooperation between adsorption and precipitation. The extent of removal of Cr(VI) decreased in the presence of PO₄³⁻, likely because of the competitive adsorption of PO₄³⁻ with Cr(VI), which existed as HCrO₄⁻ on TESM. The impact of Cl⁻ and SO₄²⁻ on the removal of Ag(I) and SO₄²⁻ on Pb(II) was similar to that of PO₄³⁻. The adsorbability of TESM for the other ions decreased, not exceeding 20% in the presence of Cl⁻, NO₃⁻, or SO₄²⁻. Considering that the tested concentration of these anions was much higher than that really present in natural waters, the inhibition of the coexisting anions for heavy metal ion adsorption on TESM was not crucial.⁴³ In addition, the adsorbability of TESM decreased slightly with an increase in HA concentration, probably because the suspended organic substances could block the pores of the adsorbents, which restrained the adsorption of heavy metal ions.⁹

Effect of Natural Water Matrices. The removal abilities of TESM with respect to Cr(VI), Hg(II), Cu(II), Pb(II), Cd(II), and Ag(I) were investigated with different water matrices (including ultrapure water, tap water, and river water) spiked with a single metal ion. The adsorption capacity of TESM for Hg(II) and Ag(I) was almost independent of the water matrix, showing the minor effect of the water matrix on removal of Hg(II) and Ag(I) (Table 2). This is probably due to the very strong affinity for Hg(II) and Ag(I).⁴⁴ However, the adsorption capacity of TESM for Cr(VI), Cu(II), Pb(II), and Cd(II) decreased in tap water and river water, as compared with that in ultrapure water, showing that water matrix could affect the performance of TESM for the removal of Cr(VI), Cu(II), Pb(II), and Cd(II). Furthermore, the TESM adsorbed more heavy metals from ultrapure water than from other water

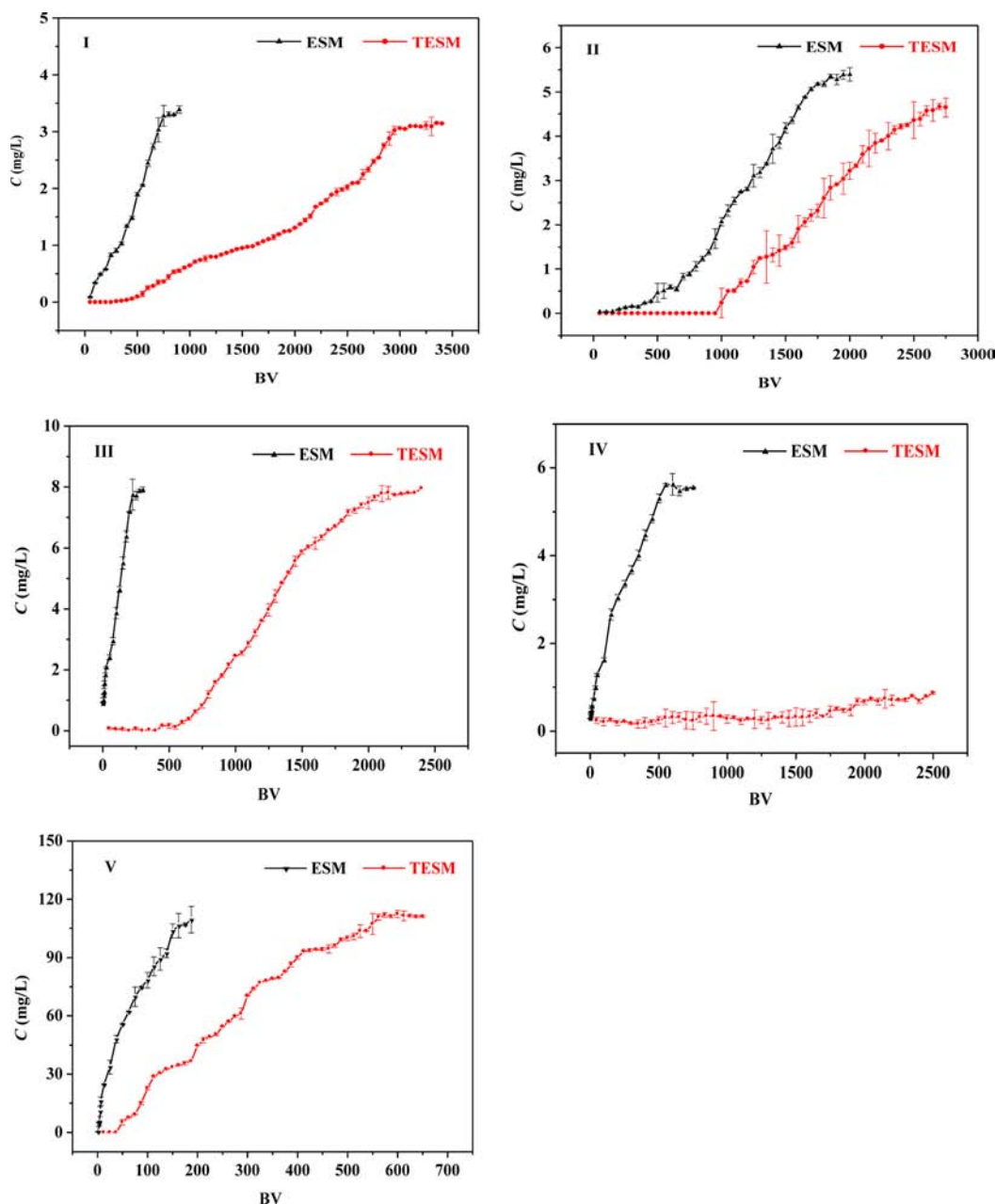


Figure 6. Breakthrough curves for TESM and ESM packed columns for different toxic heavy metal ions in real industrial wastewater at a loading flow rate of 3.0 mL/min. I–IV are the electroplating wastewaters, mainly containing 3.51 mg/L Cu(II), 5.54 mg/L Cr(VI), 8.10 mg/L Pb(II), and 5.93 mg/L Ag(I), respectively. V is the effluent of a factory producing Na_2CrO_4 , mainly containing 110.50 mg/L Cr(VI).

sources. This indicates that the various inorganic (for example, Ca^{2+} and Mg^{2+}) and organic (total organic carbon, TOC) substances in natural water could interact with the TESM adsorbent and, thus, exhibit competition with target heavy metals. The order of contents of TOC, Ca^{2+} , and Mg^{2+} in different water matrices is as follows: ultrapure water < tap water < river water (Table 2). Although their affinity for the thiol group is weak, Ca^{2+} and Mg^{2+} could still bind with a portion of the adsorption sites on the surface of TESM. The suspended organic substances could block the pores of the adsorbents, which leads to the decrease in the level of adsorption. In terms of the contents of the competing metal cations, like Ca^{2+} and Mg^{2+} , and TOC (Table 2), the order of sorption capacity of TESM for Cr(VI), Cu(II), Cd(II), and

Pb(II) in three studied water sources is as follows: ultrapure water > tap water > river water.

Regeneration and Recycling of the TESM Adsorbent.

HNO_3 (1 mol/L) was used for regeneration of the TESM adsorbent after Cu(II), Cd(II), and Pb(II) adsorption. NaOH (1 mol/L) was used for regeneration of the TESM adsorbent after Cr(VI) adsorption, and HNO_3 (1 mol/L) with 2% thiourea was used for regeneration of the TESM adsorbent after Hg(II) and Ag(I) adsorption. Our results indicate that the TESM kept >80% of its binding capacity to take up Cu(II), Cd(II), Hg(II), and Pb(II) after five cycles, indicating the high stability and good regeneration performance of TESM. This suggests that the TESM adsorbent can be used for the repeated treatment of the target toxic heavy metals. For Cr(VI), the adsorption capacity decreased to 60% because of the redox

reaction between the thiol group and Cr(VI). However, the regenerated TESM does not show a good ability to retain Ag(I). This may be due to the strong interaction between the thiol group and Ag(I), thus making it difficult to elute the adsorbed silver ions.

Breakthrough Experiments for Practical Wastewater Purification. The breakthrough point was defined on the basis of the concentration limit set by the State Standard of the People's Republic of China,⁴⁵ in which 0.5 mg/L was set for Cr(VI), Cu(II), and Ag(I) and 1 mg/L was set for Pb(II). Figure 6 shows the breakthrough curves for Cr(VI), Cu(II), Ag(I), and Pb(II) during the loading test. The curves clearly demonstrate the much higher adsorption capacity of the TESM adsorbent versus that of ESM in the column experiment. The breakthrough volumes of the TESM column were found to be 800, 1050, 750, 1750, and 37.5 BV for Cu(II), Cr(VI), Pb(II), Ag(I), and Cr(VI) in wastewaters I–V, respectively. However, for the ESM column, the breakthrough volumes were 150, 500, 2.5, 10, and 1.25 BV for Cu(II), Cr(VI), Pb(II), Ag(I), and Cr(VI) in wastewaters I–V, respectively. The breakthrough volume of the TESM column for Cr(VI) in industrial wastewater II was much higher than that in wastewater V; this is because the concentration of Cr(VI) in wastewater V is much higher than that in wastewater II. These results prove that the TESM can be used as column packing to purify real wastewater by filtration and could be promising for the removal of toxic metal ions such as Cu(II), Cr(VI), Pb(II), and Ag(I).

Adsorption Mechanism. The possible mechanism of adsorption of toxic metal ions onto the TESM biosorbent was explored. Hg(II), Ag(I), Cu(II), Cd(II), and Pb(II) all present as cations in solution and can form complexes with the thiol group because the thiol group is an excellent ligand. It was observed that TESM showed different binding capacities for various ions, and the order of adsorption capacities of the tested metal ions on TESM is as follows: Hg(II) > Ag(I) > Cu(II) > Pb(II) \approx Cd(II) (Figure 3). This can be explained by the Lewis acid–base interactions.^{18,19} Also, the formation of a complex between the target heavy metal ions and TESM can be confirmed by the obvious disappearance of the S–H stretching mode in Raman spectra after adsorption (Figure 7).

Because Cr(VI) exists as anions in the water solution, the electrostatic attraction between the negative Cr(VI) and the positive surface of the TESM adsorbent is the major adsorption mechanism. To explore more possible mechanisms of

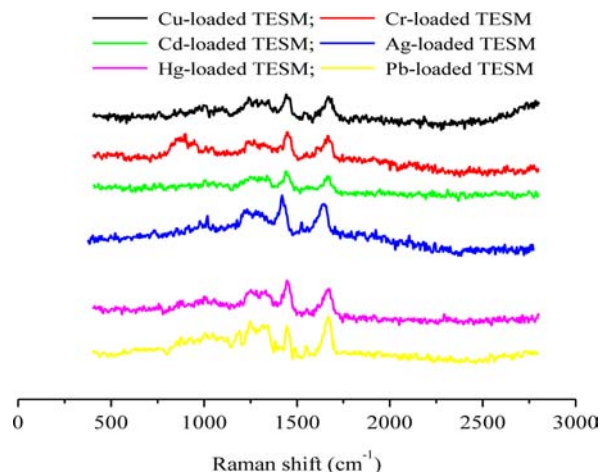


Figure 7. Raman spectra of TESM after adsorption of metal ions.

adsorption of Cr(VI) onto TESM, first, we determined the variation of the equilibrium concentration of Cr(VI) and Cr(III) in solution after reaction with TESM as a function of the initial solution pH. The results indicate that chromium has a valence change, and the reduction from Cr(VI) to Cr(III) occurs during the adsorption process (Figure 8). This suggests

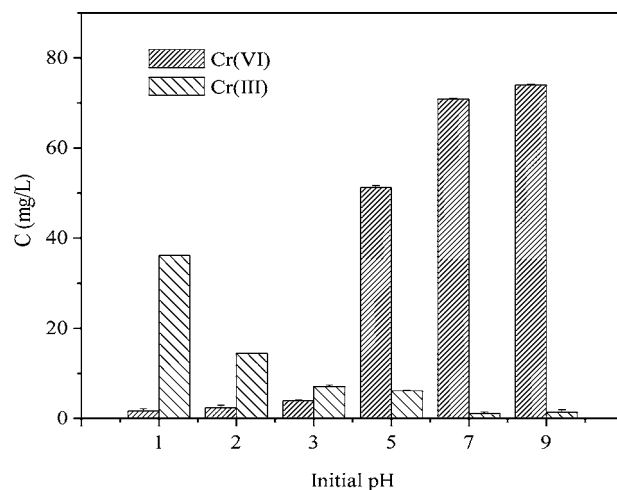


Figure 8. Equilibrium concentrations of Cr(III) and Cr(VI) at different initial pH values.

that the reduction of Cr(VI) to Cr(III) occurred during the adsorption processes, and the lower the initial pH of the mixture, the higher the concentration ratio of Cr(III) to Cr(VI) in the solution. Second, we employed an XPS study to investigate the surface chemical composition of Cr-adsorbed TESM (Figure 9). The high-resolution XPS spectrum shows two Cr 2p_{3/2} intensity peaks at 577.2 and 579.2 eV, which are consistent with Cr(III) and Cr(VI),⁴⁶ respectively. It is obvious that both Cr(III) and Cr(VI) coexist on the surface of TESM. Meanwhile, the broad peak of O 1s can be fit by three peaks at binding energies of 530.8, 532.2, and 533.5 eV. The peak around 530.8 eV represents the structural oxygen in metal oxides; the peak at 532.2 eV is characteristic of oxygen in the hydroxyl group of a metal hydroxide such as Cr(OH)₃, and the peak at 533.5 eV indicates the oxygen in the absorbed water.⁴⁷ The N atom of amine groups in the TESM is located at ~400 eV. A new peak appears after the adsorption of Cr(VI), which suggests that N atoms of the amine groups participate in the progressing adsorption,⁴⁸ and the characteristic peak of S atoms shifted from 163.4 to 168.5 eV after adsorption, which were attributed to the SH and SO₃H groups, respectively.^{49,50}

In conclusion, this study reports the synthesis of thiol-functionalized food residue eggshell membrane biomaterials by using a simple chemical reduction of disulfide bonds in ESM by ammonium thioglycolate. The experimental results demonstrate that TESM biomaterials can be used as new and efficient adsorbents for the removal of multifold toxic heavy metal ions, including Cr(VI), Hg(II), Cu(II), Pb(II), Cd(II), and Ag(I), from aqueous media. More importantly, TESM is also capable of detoxifying Cr(VI). Considering the simple synthesis procedure, low cost, high removal efficiency, and environmental friendliness, it is expected that the TESM may be a promising biosorbent for the removal of heavy metal ions from water solutions.

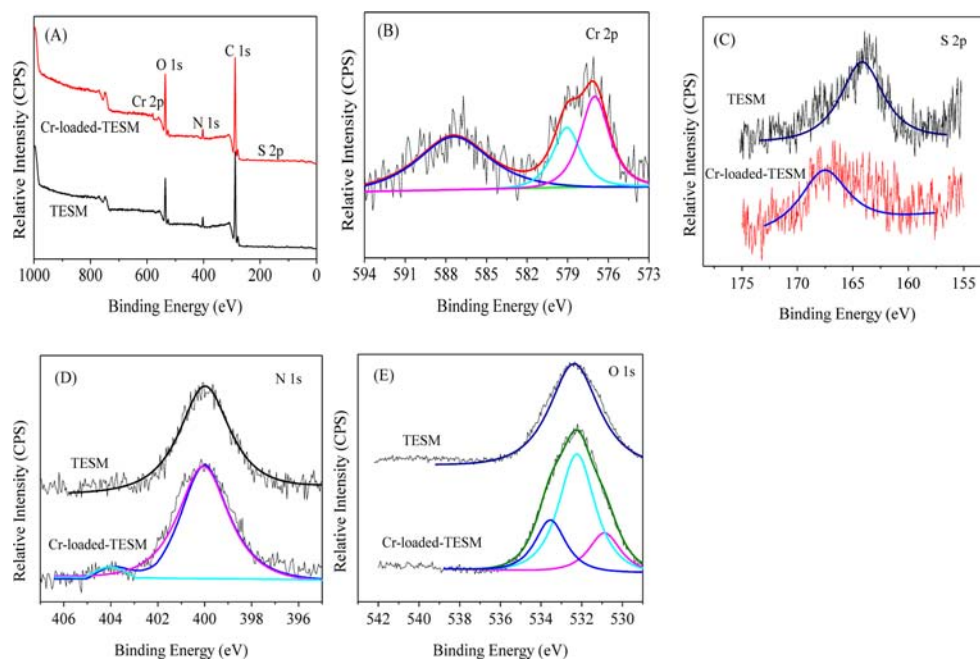


Figure 9. XPS spectra of the TESM before and after Cr(VI) adsorption: (A) survey, (B) Cr 2p, (C) S 2p, (D) N 1s, and (E) O 1s.

■ ASSOCIATED CONTENT

Supporting Information

Tables S1–S4 and Figures S1–S4. This material is available free of charge via the Internet at <http://pubs.acs.org>.

■ AUTHOR INFORMATION

Corresponding Author

*Telephone: +86-23-68254843. Fax: +86-23-68254843. E-mail: yuminghuang2000@yahoo.com.

Funding

Financial support from the National Natural Science Foundation of China (21277111) is gratefully acknowledged.

Notes

The authors declare no competing financial interest.

■ REFERENCES

- Wang, Y.; Zou, B.; Gao, T.; Wu, X.; Lou, S.; Zhou, S. Synthesis of orange-like Fe₃O₄/PPy composite microspheres and their excellent Cr(VI) ion removal properties. *J. Mater. Chem.* **2012**, *22*, 9034–9040.
- Zhu, Y.; Yu, H.; Wang, J.; Fang, W.; Yuan, J.; Yang, Z. Heavy metal accumulations of 24 asparagus bean cultivars grown in soil contaminated with Cd alone and with multiple metals (Cd, Pb, and Zn). *J. Agric. Food Chem.* **2007**, *55*, 1045–1052.
- Bordajandi, L. R.; Gómez, G.; Abad, E.; Rivera, J.; Fernández-Bastón, M. d. M.; Blasco, J.; González, M. J. Survey of persistent organochlorine contaminants (PCBs, PCDD/Fs, and PAHs), heavy metals (Cu, Cd, Zn, Pb, and Hg), and arsenic in food samples from huelva (Spain): Levels and health implications. *J. Agric. Food Chem.* **2004**, *52*, 992–1001.
- Maiga, A.; Diallo, D.; Bye, R.; Paulsen, B. S. Determination of some toxic and essential metal ions in medicinal and edible plants from Mali. *J. Agric. Food Chem.* **2005**, *53*, 2316–2321.
- Kirby, J. K.; Lyons, G. H.; Karkkainen, M. P. Selenium speciation and bioavailability in biofortified products using species-unspecific isotope dilution and reverse phase ion pairing–inductively coupled plasma–mass spectrometry. *J. Agric. Food Chem.* **2008**, *56*, 1772–1779.
- Agrawal, R. K. S. M. Biological effects of heavy metals: An overview. *J. Environ. Biol.* **2005**, *26*, 301–313.

(7) Babić, B. M.; Milonjić, S. K.; Polovina, M. J.; Čupić, S.; Kaludjerović, B. V. Adsorption of zinc, cadmium and mercury ions from aqueous solutions on an activated carbon cloth. *Carbon* **2002**, *40*, 1109–1115.

(8) Navarro, R. R.; Wada, S.; Tatsumi, K. Heavy metal precipitation by polycation–polyanion complex of PEI and its phosphonomethylated derivative. *J. Hazard. Mater.* **2005**, *123*, 203–209.

(9) Dobrevsky, I.; Dimova-Todorova, M.; Panayotova, T. Electroplating rinse waste water treatment by ion exchange. *Desalination* **1997**, *108*, 277–280.

(10) Janssen, L. J. J.; Koene, L. The role of electrochemistry and electrochemical technology in environmental protection. *Chem. Eng. J.* **2002**, *85*, 137–146.

(11) Rozada, F.; Otero, M.; Morán, A.; García, A. I. Adsorption of heavy metals onto sewage sludge-derived materials. *Bioresour. Technol.* **2008**, *99*, 6332–6338.

(12) Dawood, S.; Sen, T. K. Removal of anionic dye Congo red from aqueous solution by raw pine and acid-treated pine cone powder as adsorbent: Equilibrium, thermodynamic, kinetics, mechanism and process design. *Water Res.* **2012**, *46*, 1933–1946.

(13) Yin, P.; Wang, Z.; Qu, R.; Liu, X.; Zhang, J.; Xu, Q. Biosorption of heavy metal ions onto agricultural residues buckwheat hulls functionalized with 1-hydroxyethylidenediphosphonic acid. *J. Agric. Food Chem.* **2012**, *60*, 11664–11674.

(14) Minamisawa, M.; Minamisawa, H.; Yoshida, S.; Takai, N. Adsorption behavior of heavy metals on biomaterials. *J. Agric. Food Chem.* **2004**, *52*, 5606–5611.

(15) Peng, X. W.; Zhong, L. X.; Ren, J. L.; Sun, R. C. Highly effective adsorption of heavy metal ions from aqueous solutions by macroporous xylan-rich hemicelluloses-based hydrogel. *J. Agric. Food Chem.* **2012**, *60*, 3909–3916.

(16) Zhong, L. X.; Peng, X. W.; Yang, D.; Sun, R. C. Adsorption of heavy metals by a porous bioadsorbent from lignocellulosic biomass reconstructed in an ionic liquid. *J. Agric. Food Chem.* **2012**, *60*, 5621–5628.

(17) Boddu, V. M.; Abburi, K.; Talbott, J. L.; Smith, E. D.; Haasch, R. Removal of arsenic(III) and arsenic(V) from aqueous medium using chitosan-coated biosorbent. *Water Res.* **2008**, *42*, 633–642.

(18) Li, G.; Zhao, Z.; Liu, J.; Jiang, G. Effective heavy metal removal from aqueous systems by thiol functionalized magnetic mesoporous silica. *J. Hazard. Mater.* **2011**, *192*, 277–283.

- (19) Chai, L.; Li, Q.; Zhu, Y.; Zhang, Z.; Wang, Q.; Wang, Y.; Yang, Z. Synthesis of thiol-functionalized spent grain as a novel adsorbent for divalent metal ions. *Bioresour. Technol.* **2010**, *101*, 6269–6272.
- (20) Toro, P.; Quijada, R.; Yazdani-Pedram, M.; Arias, J. L. Eggshell, a new bio-filler for polypropylene composites. *Mater. Lett.* **2007**, *61*, 4347–4350.
- (21) Yi, F.; Guo, Z.-X.; Zhang, L.-X.; Yu, J.; Li, Q. Soluble eggshell membrane protein: Preparation, characterization and biocompatibility. *Biomaterials* **2004**, *25*, 4591–4599.
- (22) Goddard, D. R.; Michaelis, L. A study on keratin. *J. Biol. Chem.* **1934**, *106*, 605–614.
- (23) Tsai, W. T.; Yang, J. M.; Lai, C. W.; Cheng, Y. H.; Lin, C. C.; Yeh, C. W. Characterization and adsorption properties of eggshells and eggshell membrane. *Bioresour. Technol.* **2006**, *97*, 488–493.
- (24) Jing, Y. D.; He, Z. L.; Yang, X. E. Effects of pH, organic acids, and competitive cations on mercury desorption in soils. *Chemosphere* **2007**, *69*, 1662–1669.
- (25) State Standard of the People's Republic of China—Water Quality-Determination of Copper, Zinc, Lead and Cadmium-Atomic Absorption Spectrometry; GB-7475-1987; National Environmental Protection Agency, 1987.
- (26) State Standard of the People's Republic of China—Water Quality-Determination of Silver—Flame Atomic Absorption Spectrometry; GB-11907-1989; National Environmental Protection Agency, 1989.
- (27) State Standard of the People's Republic of China—Water Quality-Determination of Calcium and Magnesium-Atomic Absorption Spectrophotometric Method; GB-11905-1989; National Environmental Protection Agency, 1989.
- (28) State Standard of the People's Republic of China—Water Quality-Determination of Chromium(VI)-1,5-Diphenylcarbohydrazide Spectrophotometric Method; GB-7467-1987; National Environmental Protection Agency, 1987.
- (29) Teixeira, M. C.; Ciminelli, V. S. T.; Dantas, M. S. S.; Diniz, S. F.; Duarte, H. A. Raman spectroscopy and DFT calculations of As(III) complexation with a cysteine-rich biomaterial. *J. Colloid Interface Sci.* **2007**, *315*, 128–134.
- (30) Diaz Fleming, G.; Finnerty, J. J.; Campos-Vallette, M.; Célis, F.; Aliaga, A. E.; Fredes, C.; Koch, R. Experimental and theoretical Raman and surface-enhanced Raman scattering study of cysteine. *J. Raman Spectrosc.* **2009**, *40*, 632–638.
- (31) Lu, X.; Yin, Q.; Xin, Z.; Zhang, Z. Powerful adsorption of silver(I) onto thiol-functionalized polysilsesquioxane microspheres. *Chem. Eng. Sci.* **2010**, *65*, 6471–6477.
- (32) Parr, R. G.; Pearson, R. G. Absolute hardness: Companion parameter to absolute electronegativity. *J. Am. Chem. Soc.* **1983**, *105*, 7512–7516.
- (33) Lagadic, I. L.; Mitchell, M. K.; Payne, B. D. Highly effective adsorption of heavy metal ions by a thiol-functionalized magnesium phyllosilicate clay. *Environ. Sci. Technol.* **2001**, *35*, 984–990.
- (34) Najafi, M.; Yousefi, Y.; Rafati, A. A. Synthesis, characterization and adsorption studies of several heavy metal ions on amino-functionalized silica nano hollow sphere and silica gel. *Sep. Purif. Technol.* **2012**, *85*, 193–205.
- (35) Wang, L.; Wu, X.-L.; Xu, W.-H.; Huang, X.-J.; Liu, J.-H.; Xu, A.-W. Stable organic–inorganic hybrid of polyaniline/ α -zirconium phosphate for efficient removal of organic pollutants in water environment. *ACS Appl. Mater. Interfaces* **2012**, *4*, 2686–2692.
- (36) Zhou, J.; Tang, C.; Cheng, B.; Yu, J.; Jaroniec, M. Rattle-type carbon–alumina core–shell spheres: Synthesis and application for adsorption of organic dyes. *ACS Appl. Mater. Interfaces* **2012**, *4*, 2174–2179.
- (37) Ma, F.; Qu, R.; Sun, C.; Wang, C.; Ji, C.; Zhang, Y.; Yin, P. Adsorption behaviors of Hg(II) on chitosan functionalized by amino-terminated hyperbranched polyamidoamine polymers. *J. Hazard. Mater.* **2009**, *172*, 792–801.
- (38) Bai, L.; Hu, H.; Fu, W.; Wan, J.; Cheng, X.; Zhuge, L.; Xiong, L.; Chen, Q. Synthesis of a novel silica-supported dithiocarbamate adsorbent and its properties for the removal of heavy metal ions. *J. Hazard. Mater.* **2011**, *195*, 261–275.
- (39) Takagai, Y.; Shibata, A.; Kiyokawa, S.; Takase, T. Synthesis and evaluation of different thio-modified cellulose resins for the removal of mercury(II) ion from highly acidic aqueous solutions. *J. Colloid Interface Sci.* **2011**, *353*, 593–597.
- (40) Najafi, M.; Rostamian, R.; Rafati, A. A. Chemically modified silica gel with thiol group as an adsorbent for retention of some toxic soft metal ions from water and industrial effluent. *Chem. Eng. J.* **2011**, *168*, 426–432.
- (41) Wu, Y.-N.; Li, F.; Liu, H.; Zhu, W.; Teng, M.; Jiang, Y.; Li, W.; Xu, D.; He, D.; Hannam, P.; Li, G. Electrospun fibrous mats as skeletons to produce free-standing MOF membranes. *J. Mater. Chem.* **2012**, *22*, 16971–16978.
- (42) Mandel, K.; Hutter, F.; Gellermann, C.; SEXTL, G. Modified superparamagnetic nanocomposite microparticles for highly selective Hg^{II} or Cu^{II} separation and recovery from aqueous solutions. *ACS Appl. Mater. Interface* **2012**, *4*, 5633–5642.
- (43) Qiang, Z.; Bao, X.; Ben, W. MCM-48 modified magnetic mesoporous nanocomposite as an attractive adsorbent for the removal of sulfamethazine from water. *Water Res.* **2013**, *47*, 10.1016/j.watres.2012.10.039.
- (44) Merrifield, J. D.; Davids, W. G.; MacRae, J. D.; Amirbahman, A. Uptake of mercury by thiol-grafted chitosan gel beads. *Water Res.* **2004**, *38*, 3132–3138.
- (45) State Standard of the People's Republic of China—Integrated Wastewater Discharged Standard; GB-8978-1996; Standards Press of China: Beijing, 1996.
- (46) Fang, J.; Gu, Z.; Gang, D.; Liu, C.; Ilton, E. S.; Deng, B. Cr(VI) removal from aqueous solution by activated carbon coated with quaternized poly(4-vinylpyridine). *Environ. Sci. Technol.* **2007**, *41*, 4748–4753.
- (47) Manning, B. A.; Kiser, J. R.; Kwon, H.; Kanel, S. R. Spectroscopic investigation of Cr(III)- and Cr(VI)-treated nanoscale zerovalent iron. *Environ. Sci. Technol.* **2007**, *41*, 586–592.
- (48) Jin, L. Mechanisms of lead adsorption on chitosan/PVA hydrogel beads. *Langmuir* **2002**, *18*, 9765–9770.
- (49) Shevchenko, N.; Zaitsev, V.; Walcarius, A. Bifunctionalized mesoporous silicas for Cr(VI) reduction and concomitant Cr(III) immobilization. *Environ. Sci. Technol.* **2008**, *42*, 6922–6928.
- (50) Ganesan, V.; Walcarius, A. Surfactant templated sulfonic acid functionalized silica microspheres as new efficient ion exchangers and electrode modifiers. *Langmuir* **2004**, *20*, 3632–3640.